Mathematical and Experimental Verification of Efficient Force Transmission by Biarticular Muscle Actuator

Sehoon Oh * **Valerio Salvucci** * **Yasuto Kimura** ** **Yoichi Hori** **

* *Department of Electrical Engineering, University of Tokyo, 3-7-1 Hongo Bunkyoku Tokyo, Japan (e-mail:sehoon,valerio@hori.k.u-tokyo.ac.jp)*
** *Department of Advanced Energy, University of Tokyo, 5-1-5 Kashiwanoha Kashiwa Chiba, Japan (e-mail:kimura@hori.k.u-tokyo.ac.jp,hori@k.u-tokyo.ac.jp)*

Abstract: This paper proves that the biarticular muscle structure which is common in most of animals improves the force generation efficiency in a two-link manipulator. To this end, the statics of two configurations - two joint-actuators configuration and one joint-actuator and one biarticular actuator configuration - are compared using two types of Jacobian. Moreover, the statics are simplified to clarify this difference and an analytical solution about the efficiency of the biarticular muscle structure is proposed. Finally, experimental results verify this advantage of the biarticular muscle structure.

Keywords: Robots manipulators, Modeling, Mechatronic systems

1. INTRODUCTION

The biarticular muscle is an intrinsic mechanism that is shared by most of animals from the lancelet (Tsuji [2010]) to our human. Even though the biarticular muscle mechanism is such a fundamental mechanism, it has been neglected in the design of robots. However, it has started to be highlighted again in robotics recently (Tsuji [2010], Iida [2008], Klein [2008], Hosoda [2010], Niiyama [2010]).

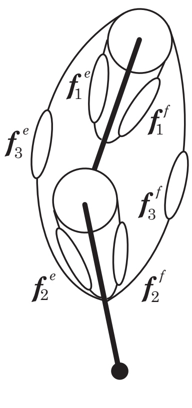

Fig. 1. Two-Joint Structure with Muscle Model

Figure 1 shows the 3 pairs of muscles: flexors and extensors of two monoarticular muscle pairs ($f_1^{\{e,f\}}, f_2^{\{e,f\}}$) and one biarticular muscle pair ($f_3^{\{e,f\}}$). The monoarticular muscles are connected around only one joint generating a torque on the joint, while the biarticular muscles are connected across two joints providing torques to two joints at the same time.

⋆ This work was supported in part by the Inamori Foundation

This biarticular muscle structure was introduced to the robotics several decades ago (Hogan [1985]), but it was not fully applied to robotics. Recent research, however, proves that in spite of the redundancy, the biarticular muscle has many advantages and can improve control of humanoid robots (Iida [2008], Klein [2008], Hosoda [2010], Niiyama [2010]).

In the physiology, the biarticular muscle is said to play a significant role making power transfer in human motions (Jacobs [1996], Schenau [1987]). Three pairs of muscles activated in an antagonistic way with a phase difference can generate a well-shaped force hexagon at the endeffector providing a simplified force generation (Kumamoto [1994]).

In the robotics, the biarticular muscle is adopted to develop robots that mimic animals (Tsuji [2010],Niiyama [2007]) showing that the biarticular muscle can simplify motion control.

However, these advantages of the biarticular muscle have been shown only in empirical ways, until we developed a novel statics based on the biarticular muscle system and clarified the simplification by the biarticular muscle system in a numerical way (Oh [2009]).

Based on this simple statics, we could suggest a novel feedback control which can control the direction of the reaction force at the endeffector without any force feedback (Oh [2010]). This could be achieved due to the simplicity in the statics of the biarticular muscle structure.

Recently, we also have proved that the biarticular muscle can distribute the necessary torques for the desired forces at the endeffector in an optimal way (Valerio [2010]), and it coincides with the physiological data of human subjects (Kumamoto [1994]).

In spite of these advantages, there still is a question about whether a robot really needs the biarticular muscle actuator. This paper addresses this problem proving the biarticular muscle has more efficient torque transmission characteristics. To clarify this point, the statics of a two-link manipulator with two different configurations (two joint-torques configuration and one monoarticular muscle torque on the first joint and the biarticular muscle torque configuration) are analyzed and compared in this paper.

First, in Section 2 we compare the required torques to generate a constant force at the endeffector in a numerical way using Jacobian. Then in Section 3, a simple representation way of the statics for a general two-joint manipulator is derived as another comparison tool. Finally, in Section 4 efficiency of the biarticular muscle actuator is verified using experiments.

2. COMPARISON OF THE STATICS BETWEEN JOINT ACTUATOR AND BIARTICULAR MUSCLE ACTUATOR

2.1 Configuration of a two-link manipulator driven by joint actuators and biarticulated actuator

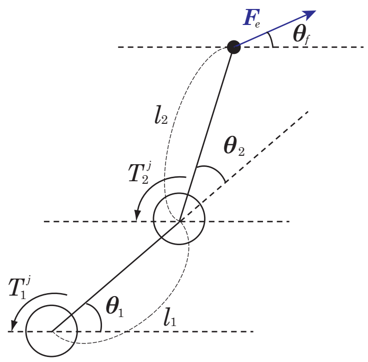

Fig. 2. Configuration of Two-link Manipulator

Figure 2 is the configuration of a two-link manipulator, where two actuators are located in two joints, while Figure 3 illustrates another type of a two-link manipulator with a biarticular muscle actuator represented by a linear motor. The muscle torques that are generated by $f_i^{e,f}$ in Figure 1

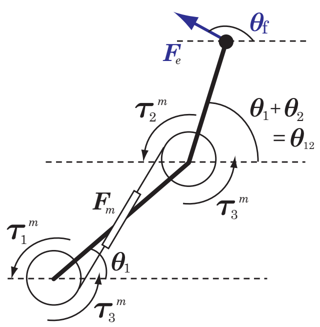

Fig. 3. Configuration of Two Degree-of-freedom Planar Manipulator with Biarticular Muscle

is described as τ_i^m in Figure 3.

The biarticular muscle structure is embedded in various ways in the robotics. Yoshida [2009] and Tsuji [2010] use the pulleys to transmit a torque generated by a motor to two joints, Iida [2008] and Klein [2008] use the springs, and Hosoda [2010] and Niiyama [2010] use the McKibben muscles as passive actuators for the biarticular muscle. Planatery gears are also used to realize the biarticular muscles (Umemura [2010], Kimura [2010]). Fujimoto [2010] develops a small linear actuator that can work as a biarticular muscle, which is illustrated in Figure 3. A linear force F_m can produce a torque τ_3^m in two joints working as a biarticular muscle actuator.

Even though there are various realization ways, they share a common point; the torque generated by the biarticular muscle actuator affects two joints at the same time. In this paper, this characteristic is described using the muscle torque representation; τ_1^m, τ_2^m are the torques generated by monoarticular muscles force of two joints $f_1^{e,f}, f_2^{e,f}$, and τ_3^m is the torque generated by a biarticular muscle force $f_3^{e,f}$ in Figure 1. For the comparison, the torques of joint actuators in Figure 2 are represented as T_1^j and T_2^j in this paper.

Under this description, the relation between these two kinds of torques is defined as the following.

$$\begin{pmatrix} T_1^j \\ T_2^j \end{pmatrix} = \begin{pmatrix} \tau_1^m + \tau_3^m \\ \tau_2^m + \tau_3^m \end{pmatrix} \tag{1}$$

2.2 Statics expressed by two types of Jacobian

The statics that represents the balance between force generated at the endeffector and the applied joint torques is usually described using Equation (2) where force F_e in Figure 2 is described as $\boldsymbol{F}_e = (f_x, f_y)^T$.

$$\begin{pmatrix} T_1^j \\ T_2^j \end{pmatrix} = J^T \begin{pmatrix} f_x \\ f_y \end{pmatrix} \tag{2}$$

$$J = \begin{pmatrix} -l_1 \sin\theta_1 - l_2 \sin(\theta_1+\theta_2) & -l_2 \sin(\theta_1+\theta_2) \\ l_1 \cos\theta_1 + l_2 \cos(\theta_1+\theta_2) & l_2 \cos(\theta_1+\theta_2) \end{pmatrix} \tag{3}$$

Now we define the statics for the muscle actuator configuration in Figure 3. However there is a redundancy - three torques to generate two dimensional force. In order to deal with this problem, we intentionally ignore the second monoarticular muscle torque τ_2^m.

There is another reason to ignore τ_2^m. By removing τ_2^m, the comparison we address here becomes clear; when we are given two actuators, which configuration is more efficient for a two-link manipulator, two joint-actuators configuration where two joint torques T_1^j and T_2^j generate F_e or one joint motor and one biarticular motor configuration where one monoarticular muscle torque τ_1^m and one biarticular muscle torque τ_3^m generate the force? This configuration difference can be illustrated as Figure 4 and 5.

Under this τ_1^m, τ_3^m configuration (Figure 5), the torques necessary to generate the force F_e can be described as follows Oh [2009].

$$\begin{pmatrix} \tau_1^m \\ \tau_3^m \end{pmatrix} = \begin{pmatrix} 1 & -1 \\ 0 & 1 \end{pmatrix} \begin{pmatrix} T_1^j \\ T_2^j \end{pmatrix}$$

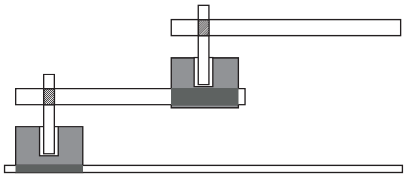

Fig. 4. Two Link Manipulator with Two Joint-motors

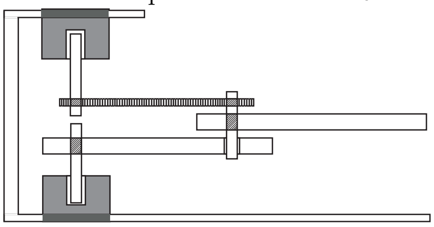

Fig. 5. Two Link Manipulator with One Joint-motor One Biarticular Motor by the Pulley

$$= \begin{pmatrix} 1 & -1 \\ 0 & 1 \end{pmatrix} J^T \begin{pmatrix} f_x \\ f_y \end{pmatrix} = (J_{abs})^T \begin{pmatrix} f_x \\ f_y \end{pmatrix},$$

where J_{abs} stands for the absolute angle Jacobian described as the following equation.

$$J_{abs} = \begin{pmatrix} -l_1 \sin\theta_1 & -l_2 \sin\theta_{12} \\ l_1 \cos\theta_1 & l_2 \cos\theta_{12} \end{pmatrix} = J \begin{pmatrix} 1 & 0 \\ -1 & 1 \end{pmatrix} \quad (5)$$

θ_{12} is defined as $\theta_1 + \theta_2$.

2.3 Comparison of required torques for the force at the endeffector

Based on two types of Jacobian introduced in the last section, necessary torques to generate a certain force at the endeffector are analyzed and compared between two cases. A force circle is adopted as a general force task. Torques to generate a force circle is calculated based on Equation (2) and (4). Figure 6 is the calculation result.

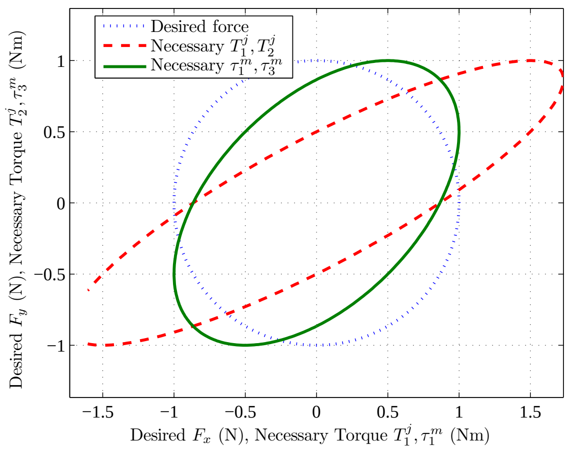

Fig. 6. Desired Force and Necessary Torques ($\theta_2 = \frac{1}{3}\pi$)

The lengths of two links l_1, l_2 are set same to $1m$, θ_2 is set to $\frac{1}{3}\pi$ and θ_1 to 0 to make the comparison easier.

The maximum necessary torques to generate 1N force at the endeffector are different in two cases. In the case of the biarticular muscle actuator which is represented by the green solid line, the maximum for the two actuators is the same 10Nm. On the other hand, in the case of the two joint-actuators that is represented by the red dashed line, the maximum for T_1^j is more than 1.73Nm. This means we need a bigger actuator to generate the same force, when we use the two joint-actuator configuration.

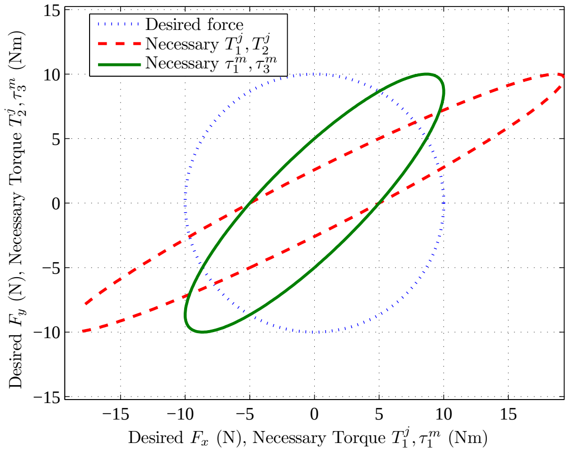

Fig. 7. Desired Force and Necessary Torques ($\theta_2 = \frac{1}{6}\pi$)

Figure 7 is the necessary torques with $\theta_2 = \frac{1}{6}\pi$. The maximum of T_1^j is around 1.93Nm, which shows the less θ_2 is, the larger T_1^j torque becomes necessary. In a two-link manipulator that is supposed to work with various posture, the actuator for T_1^j needs to have substantial torque output in order to deal with a force task under a small θ_2 condition. On the other hand, with the biarticular muscle configuration, we can fully utilize the torques of two actuators regardless of θ_2.

3. ANALYTICAL COMPARISON BY SIMPLIFIED STATICS EXPRESSION

3.1 Derivation of simplified statics

Since J_{abs} that describes the statics of the biarticular muscle configuration is fit for rotation transformation, the relationship between $\boldsymbol{F}_e$ and τ_1^m, τ_3^m can be more simplified when $\boldsymbol{F}_e$ are given as $\boldsymbol{F}_e = (F\cos\theta_f, F\sin\theta_f)$ (Oh [2009]).

$$\begin{pmatrix} \tau_1^m \\ \tau_3^m \end{pmatrix} = (J_{abs})^T \begin{pmatrix} F\cos\theta_f \\ F\sin\theta_f \end{pmatrix} = \begin{pmatrix} Fl_1 \sin(\theta_f - \theta_1) \\ Fl_2 \sin(\theta_f - \theta_{12}) \end{pmatrix} \quad (6)$$

In order to simplify Equation (6) more, the reference frame can be set along with the first link so that θ_1 can be set to 0 without loss of generality, which makes Equation (6).

$$\begin{aligned} \tau_1^m &= Fl_1 \sin\theta_f \\ \tau_3^m &= Fl_2 \sin(\theta_f - \theta_2) \end{aligned} \quad (7)$$

Using this simplified τ_1^m, τ_3^m, the statics in Equation (2) can also be transformed into the trigonometric functions. By substituting the required muscle torque in Equation (7) to Equation (1), the statics in Equation (2) is expanded as the following.

$$T_1^j = Fl_1 \sin\theta_f + Fl_2 \sin(\theta_f - \theta_2)$$
$$T_2^j = Fl_2 \sin(\theta_f - \theta_2), \quad (8)$$

This statics can also be more simplified as follows using the combination of sine functions with the parameters of l_m and θ_m defined as Figure 8. Detailed derivation process is explained in Oh [2011].

$$T_1^j = Fl_m \sin(\theta_f - \theta_m)$$
$$T_2^j = Fl_2 \sin(\theta_f - \theta_2) \quad (9)$$

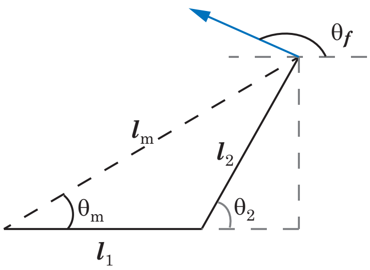

Fig. 8. Parameters for Statics of Two-link Manipulator

3.2 *Efficient force generation by biarticular muscle actuator*

The comparison done in Section 2.3 using Jacobian can be revisited using the suggested simplified statics. Figure 9 is the required torques T_1^j and T_2^j in order to generate a force of 1N at the endeffector with the direction of θ_f under the configuration $l_1 = l_2 = 1m$, $\theta_2 = \frac{\pi}{3}$. Necessary torques are illustrated with regard to the angle θ_f.

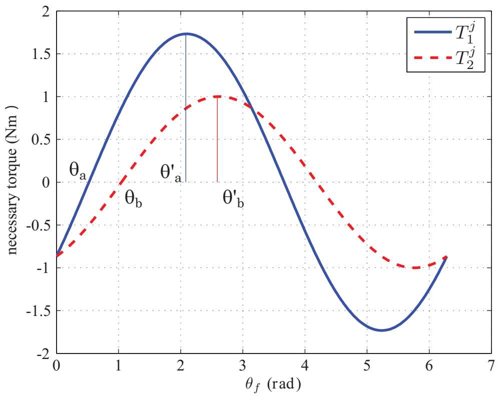

Fig. 9. Necessary Torques to Generate a Force at the Endeffector

This figure provides some general points that can be revealed only by this simplified statics. $T_1^j = T_2^j$ when the force direction θ_f is set to 0 (which is the direction of the first link) regardless of the parameters l_1, l_2, θ_2, since $l_m \sin\theta_m$ is same as $l_2 \sin\theta_2$ as is shown in Figure 8. There are four specific angles $\theta_a, \theta_b, \theta'_a, \theta'_b$; $\theta_a (= \theta_m)$ is the angle where T_1^j cannot contribute to the force at the endeffector since the moment arm of the torque T_1^j is zero (Figure 10 explains this characteristic), $\theta_b (= \theta_2)$ is the same angle for the case of T_2^j, while $\theta'_a (= \frac{\pi}{2} + \theta_m)$ is the angle where T_1^j

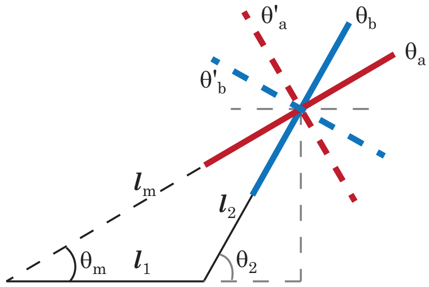

Fig. 10. Specific Angles in Force Exertion of Two Joint-actuator Manipulator

contribute most to the force and $\theta'_b (= \frac{\pi}{2} + \theta_2)$ is the same angle for T_2^j.

Figure 10 shows these angles in terms of the robot configuration; θ_a is same with θ_m, the direction in which the first joint and the endeffectors are aligned and θ_b is identified with θ_2, the direction of the second link. θ'_a and θ'_b are the angles $\frac{\pi}{2}$ away from θ_a and θ_b. This relationship is in good agreement with the explanation of Figure 9.

Magnitude Fl_m and Fl_2 in Equation (9) explain the drawback of the joint actuator configuration. Fl_m changes with regard to θ_2 as in Figure 10. In the range of $0 \leq \theta_2 \leq \frac{2\pi}{3}$, l_m is greater than l_2 (under the assumption $l_1 = l_2$) which means larger torque is required for T_1^j than T_2^j. When $\theta_2 \geq \frac{2\pi}{3}$, smaller T_1^j is good enough to generate a specific force at the endeffector.

This point is the significant difference between the statics strategies of the general two joint-actuators manipulator and the biarticulated actuator manipulator. Compared with Equation (9), the magnitudes of the necessary torques are constant in Equation (7). This implies that the output of the actuator installed in the first joint can be utilized efficiently regardless of θ_2, with the biarticular muscle actuator; the biarticular muscle torque can improve the efficiency of the actuators in terms of the force generation.

For example, in the worst case where θ_2 is set to 0, the maximum torque required for T_1^j is $F(l_1 + l_2)$, while the maximum torque required for τ_1^m is still Fl_1 to generate the same force at the endeffector.

4. VERIFICATION OF EFFICIENCY OF BIARTICULAR MUSCLE ACTUATOR BY EXPERIMENTS

4.1 *Experimental setup*

Six motors are used to realize the six muscles in Figure 1. Figure 11 is the side view of our experimental setup which shows the 6 motors. The outputs of the motors are connected to the two links through wires and pulleys. The lengths of two links are 0.112m all, and the radius of the pulleys is 22mm.

Two types of experiments are conducted. In the first experiment, the torque patterns to generate a force circle at the endeffector are given to each motor and the input torques and the output force obtained. In the second experiment, the force is measured with one pair of motor torques fixed while the other pair of motor output varies

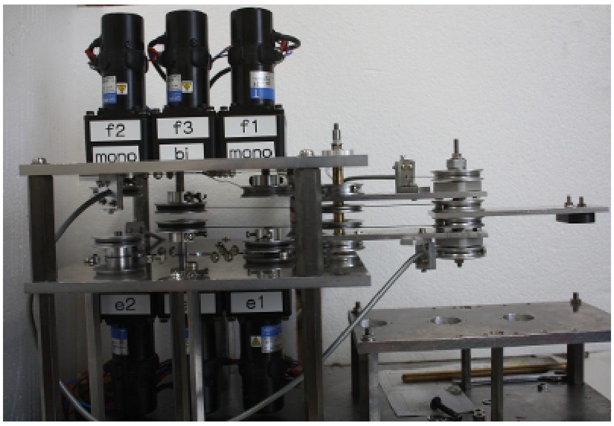

Fig. 11. 6 Motors to Mimic 6 Muscles

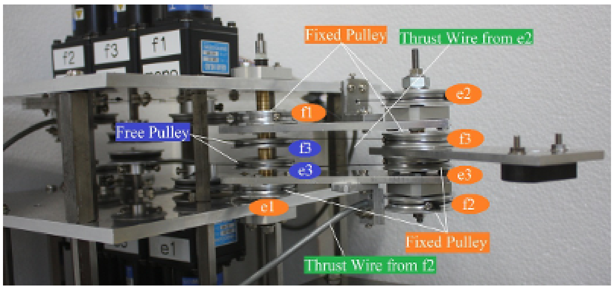

Fig. 12. Links Connected to Motors via Wires and Pulleys

so that it clarifies the relationship between torques and force.

4.2 Necessary torques to generate a certain pattern of force

In order to evaluate static force, the endeffector is constrained and connected to a force sensor. The configuration and coordinate is explained in Figure 13. The measured force is described according to this frame and θ_1 in this coordinate is not 0 anymore.

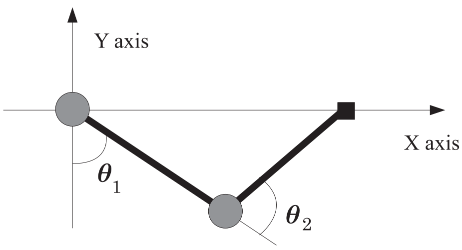

Fig. 13. Orientation of Manipulator and Force Sensor

In order to get a force circle with the magnitude of 9N, the torque patterns of T_1^j, T_2^j according to Equation (9) and the patterns of τ_1^m, τ_3^m according to Equation (7) are given in each configuration with $F = 9$. θ_2 is set to $\frac{1}{3}\pi$. 36 points of θ_f from 0 to 2π are chosen, and the converged forces are measured with each θ_f. Figure 14 and 15 are the results where the red circles are the desired force and the blue stars are measured force.

Even though there are some errors due to the transmission losses in the wires, the forces can be generated as desired. According to the coordinate definition in Figure 13, the vertical y axis corresponds the angle a' in Figure 9 where the biggest T_1^j torque is necessary. Figure 14 and 15 verify that the biarticular muscle configuration can generate the same force with less torque output from the motor.

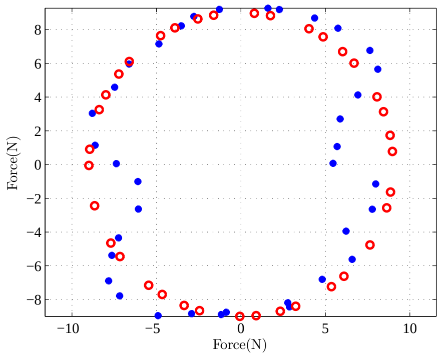

Fig. 14. Force Circle Obtained by T_1^j, T_2^j Torques

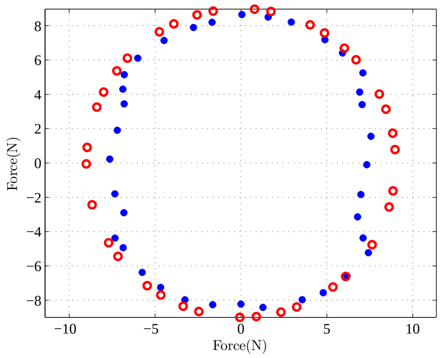

Fig. 15. Force Circle Obtained by τ_1^m, τ_3^m Torques

4.3 Comparison of force generations by joint actuator and biarticular muscle actuator

Different torque patterns are given here. First the torque for the first joint (T_1^j and τ_1^m) is fixed and the other torque (T_2^j and τ_3^m) is given from 0 to the same value of the first joint torque. The measured force is shown in Figure 16. Secondly, T_2^j and τ_3^m are fixed and the first joint torque changes from 0 to the same value of the other torque. Figure 17 is the result. θ_2 is set to $\frac{1}{6}\pi$.

The red circles are of the two joint-actuators configuration and the blue stars are of the biarticular muscle motor configuration. Lines are simulation results calculated from the suggested statics. Figure 16 indicates that T_2^j cannot contribute any force in the y direction in which direction the largest torque is necessary for T_1^j while τ_3^m can. In Figure 17, even though the torques are same in T_2^j and τ_3^m, the force in the y direction starts from the different positions, which means τ_3^m can contribute the force generation to where the first link torque needs to be large, resulting in the efficient force generation in all direction.

5. CONCLUSIONS

Here, the statics of a two-link manipulator under two different configurations - two joint-actuators configuration

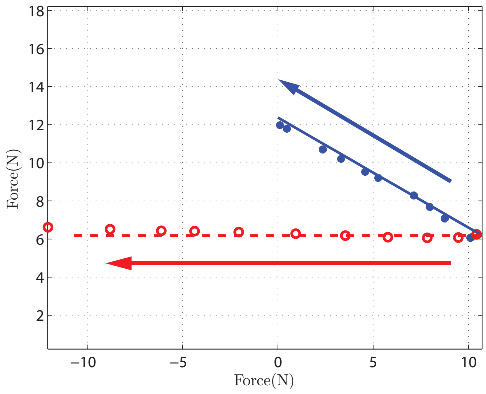

Fig. 16. Force with Varying T_2^j and τ_3^m

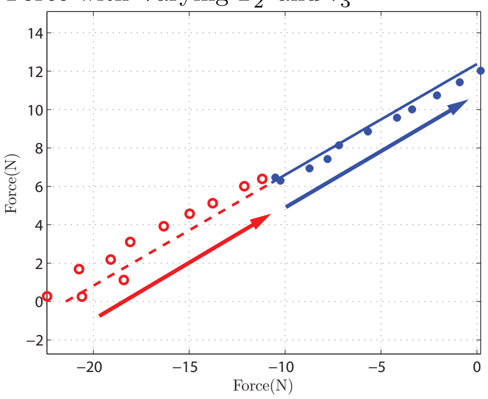

Fig. 17. Force with Varying T_1^j

and one joint motor and one biarticular muscle actuator configuration - are analyzed in a mathematical way and by several experiments.

The results show that the configuration with two joint-actuators has a drawback that it needs to have a large actuator for the first joint to generate a certain force, while the biarticular muscle configuration does not. The necessary maximum torque for the first joint is kept constant in the biarticular muscle configuration regardless of θ_2. On the other hand, it changes leading to larger torque requirement in a certain range of θ_2 in the two joint-actuator configuration.

As is said in Section 1, the advantage of the biarticular muscle is not only this efficient force generation. The biarticular muscle robotics must be a significant topic that should be studied more.

REFERENCES

Tsuji, T. A model of antagonistic triarticular muscle mechanism for lancelet robot *Proc. of IEEE Workshop on Advanced Motion Control*, 2010, pp. 496-501.

Iida, F., Rummel, J., and Seyfarth, A. Bipedal walking and running with spring-like biarticular muscles. *Journal of Biomechanics*, vol. 41, no. 3, 2008, pp. 656-667

Klein, T.J. and Lewis, M.A. On the Design of Walking Machines Using Biarticulate Actuators. *Advances in Mobile Robotics*, 2008, pp 229-237.

Hosoda, K., Sakaguchi, Y., Takayama, H. and Takuma, T. Pneumatic-driven jumping robot with anthropomorphic muscular skeleton structure. *Autonomous Robots*, vol. 28, no. 3, 2010, pp. 307 - 316.

Niiyama, R. and Kuniyoshi, Y. Design Principle Based on Maximum Output Force Profile for a Musculoskeletal Robot. *Industrial Robot: An International Journal*, vol. 37 no. 3, 2010, pp.250 - 255

Hogan, N. Impedance Control: An Approach to manipulation: Part II - Implementation. *Journal of Dynamic Systems, Measurement, and Control*, vol. 107, 1985, pp. 8-16.

Jacobs, R., Bobbert, M.F. and Schenau, GJ. van Ingen. Mechanical output from individual muscles during explosive leg extensions: the role of biarticular muscles. *Journal of Biomechanics*, vol.29, no.4, 1996, pp.513-523.

Schenau, G.J. van Ingen, Bobbert, M.F. and Rozend, R.H. The unique action of bi-articular muscles in complex movements. *Journal of Anatomy*, vol.115, 1987, pp.1-5.82.

Kumamoto, M., Oshima, T. and Yamamoto, T. Control properties induced by the existence of antagonistic pairs of bi-articular muscles - mechanical engineering model analyses. *Human Movement Science*, vol. 13, 1994, pp. 611-634.

Niiyama, R., Nagakubo, A. and Kuniyoshi, Y. Mowgli: A bipedal jumping and landing robot with an artificial musculoskeletal system. *Proc. of IEEE International Conference on Robotics and Automation*, 2007, pp.2546-2551.

Oh, S. and Hori, Y. Development of novel two-degree-of-freedom control for robot manipulator with biarticular muscle torque. *Proc. of American Control Control*, 2009, pp.325-330.

Oh, S., Kimura Y. and Hori, Y. Reaction force control of robot manipulator based on biarticular muscle viscoelasticity control. *Proc. of IEEE/ASME Advanced Intelligent Mechatronics*, 2010, pp. 1105-1110.

Salvucci, V., Oh, S and Hori, Y. Infinity norm approach for precise force control of manipulators driven by bi-articular actuators. *Proc. of Annual Conference of the IEEE Industrial Electronics Society*, 2010, pp.1908 - 1913 .

Yoshida, K., Uchida, T., Oh, S. and Hori, Y. Experimental verification on novel robot arm equipped with bi-articular driving mechanism. *Proc. of IEEE International Symposium on Industrial Electronics*, 2009, pp.1001-1006.

Fujimoto, Y., Wakayama Y., Omori, H. and Smadi, I.A. On a high-backdrivable direct-drive actuator for musculoskeletal bipedal robots. *IEEE International Workshop on Advanced Motion Control*, 2010, pp. 389-395.

Shinohara, M., Umemura, A., Haneyoshi, T. and Saito, Y. Coordination control of bi-articular robotic arm by motor drive with planetary gear. *Proc. of International Power Electronics Conference*, 2010, pp. 2551 - 2556.

Kimura, Y., Oh, S. and Hori, Y. Novel robot arm with bi-articular driving system using a planetary gear system and disturbance observer. *Proc. of IEEE International Workshop on Advanced Motion Control*, 2010, pp. 296 - 301.

Oh, S. ,Salvucci, V. and Hori, Y. Development of Simplified Statics of Robot Manipulator and Optimized Muscle Torque Distribution based on the Statics *American Control Control*, 2011, (to be presented).